Nanotechnology Perceptions
ISSN 1660-6795
www.nano-ntp.com

High-Resolution Imaging of a Complex Moving Target for Higher-Order Phase Terms Using a Novel Technique

Anitha.G[1], Karuna Kumari.K[2]

[1]Assistant Professor, Dept of EECE, GST, GITAM Deemed to be University, Visakhapatnam, A.P, India.
[2]Associate Professor, Dept of EECE, GST, GITAM Deemed to be University, Visakhapatnam, A.P, India.
Email: aguttave@gitam.edu

High-resolution radar (HRR) imaging of moving targets can be modeled as uniform, second, third, and higher-order phase terms. cubic chirps. The sea state, wave height, and wind speed are all important factors to take into account while visualizing a target-like ship. In these circumstances, the phase of the radar return signal fluctuates as it moves through the second, third, and higher orders. In this research, a novel technique using ISAR is employed for imaging with high resolution that works exceptionally well even in scenarios of maneuvering targets. Comparing the suggested algorithm to all earlier techniques demonstrates its superiority. The simulation uses a 4-point target and ship target and the results support the viability of the suggested algorithm.

Keywords: ISAR, HRR, CRR, DRR, MFCFT.

1. Introduction

HRR imaging of moving targets like ships, missiles, and airplanes in a 2D plane is implemented through ISAR. To produce a high-resolution image in 2D, the two dimensions, namely Down Range (DR) and Cross Range (CR), should have high resolution. The downrange resolution depends on the transmitted pulse width and is given by

$$DRR = \frac{cT}{2} \tag{1}$$

where c - the speed, and T -width of the pulse. The CRR depends upon the angular velocity and is given by

$$CRR = \frac{\lambda}{2\omega T_s} \tag{2}$$

where λ is the wavelength, ω is the angular speed, and T_s is the synthesis time. The fundamental RD approach is used to obtain the image of targets moving uniformly [1]. In the case of targets with complex motions, this method fails to produce images with high resolution.

Proposed [2]-[5] for maneuvering targets' ISAR imaging for second-order phase terms, the RID algorithm consists of two types. The first is the parametric method, which estimates the instantaneous Doppler frequency by modeling the received signal as an LFM signal. Nevertheless, the computational burden of these approaches is significant since they require precise calculations for each scatterer in the target [2]. The second category consists of nonparametric techniques in which the azimuth Fourier transform in the basic method is substituted by time-frequency distribution analysis tools as the Clean Technique, S-method, [3], Wigner-Ville distribution [4], and smoothed pseudo WVD [5]. Nevertheless, these methods are hindered by limited time-frequency resolution or cross-term interferences. ISAR imaging has been centered on maneuvering targets. When modeling radar doppler echoes of objects with extremely complex movements, such as roll, pitch, and yaw, the signals must be represented as third-order terms. To achieve cross-range resolution is accomplished by employing the RIC technique, which is based on the scatter instantaneous chirp rate [6]. As a result, higher-order phase term signal processing is crucial for ISAR imaging. Here, a new approach is put forth to generate HRR images of complicated targets for higher-order phase terms. By using this method, a high-resolution image is generated where all the hot spots are clearly identified.

2. METHODS IN ISAR IMAGING

When a target is rotating smoothly and each scatterer's Doppler frequency(DF) is not changing over time, the RD method is utilized. Here, the Radar continuously broadcasts the signal toward the target, which reradiates echo towards the Radar from different positions of the target [1]. All echoes are gathered to create Range profiles, and a 2D image is created by applying FFT to each profile. It is clearly explained with a diagram as shown in Fig.1.

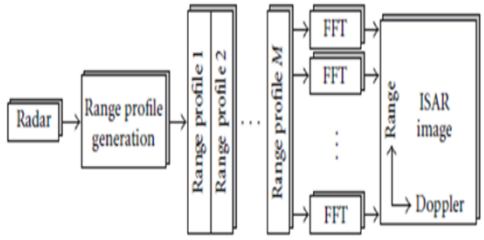

Fig.1. RD Algorithm

The RID approach is used when the target spins unevenly because this causes the DF of each scatter to change over time. The locations of the scatters in each range cell that match their instantaneous Doppler frequencies are depicted here [2-3]. This frequency depends on the

target's rotational speed during the imaging time instant as well as the precise location of the scatter. In this situation, every motion including pitch, roll, and yaw will be considered. Fig.2. shows a ship target.

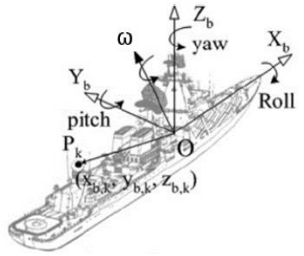

Fig.2. Ship motions

When a target is extremely maneuverable, the instantaneous speed changes over time and its rotational velocity may occasionally be very low. In such cases, the RID method has poor resolution, and some additional information is required for target identification. This can be achieved by using the RIC technique [7-10]. In RIC, a high instantaneous chirp rate frequently manifests simultaneously with RID imaging. Therefore, when the scatters have low instantaneous DF, this chirp rate of the scatter may yield a high CRR for the target. This situation is explained in Figures 3&4 which bring out the comparison between RID and RIC Techniques, where the former shows that, at some time instants, the Doppler frequency is minimum (almost zero). For example, in Fig.3, at an instant of 8s, the DF is minimum. So, in these instances of time, it is difficult to obtain the RID image. Therefore, as shown in Fig.4., at the same instant of time, the derivative of the chirp rate, is considered, where the value is not the least like the previous case.

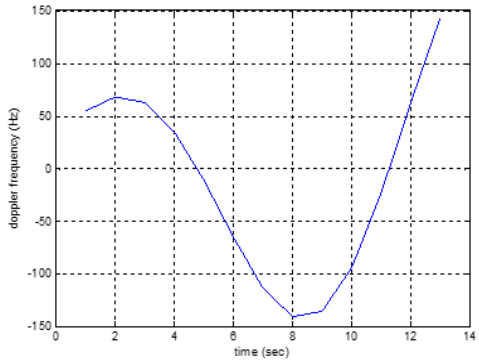

Fig .3. Doppler frequency versus Time

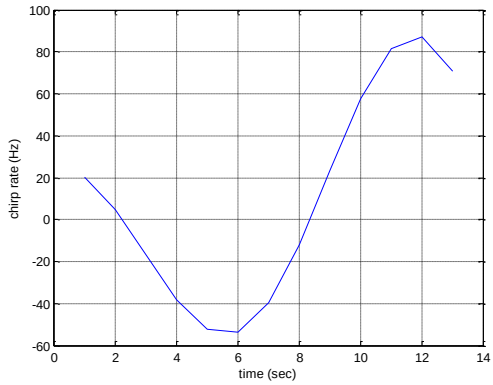

Fig.4.Chirp Rate versus Time

However, the RID method might not be useful for identifying targets for those moving at irregular speeds and with very low rotational velocities. In that situation, the RIC approach is applied, which integrates the signal coherently by using a higher-order phase signal model for each scatterer [7-10].

3. MODELING FOR HIGHER ORDER TERMS

The transmitted linear frequency-modulated signal is depicted by [7]

$$S(t_f, t_s) = rect\left(\frac{t_f}{T}\right) e^{\left(j2\pi\left(f(t)+\frac{1}{2}\gamma(t)^2\right)\right)} \quad (3)$$

where t is the total time given as $t=t_f+t_s$, and $t_s= n/prf$, (n=0,1,…N-1), N is total no of pulses, f -frequency, γ - chirp rate. The echo signal is given by

$$S_h(t_f, t_s) = \sigma_h rect\left(\frac{t_f - 2R_h(t_s)/c}{T}\right) e^{\left(j2\pi\left(f\left(t-2R_h(t_s)/c\right)+\frac{1}{2}\gamma\left(t-2R_h(t_s)/c\right)^2\right)\right)} \quad (4)$$

where σ_h is the reflection coefficient, $R_h(t_s)$ is the difference between the h^{th} scatter and radar at t_s. Keystone formatting is used for this received signal to eliminate range cell movement. If there are 'H' scatterers, then the discrete expression of equation (4) given by S(n) as

$$S(n) = \sum_{h=1}^{H} A_h W_{N_f}^{f_h n+\left(\frac{\gamma_h}{N_f}\right)n^2+\left(\frac{\beta_h}{N_f^2}\right)n^3+\left(\frac{\phi_h}{N_f^3}\right)n^3} \quad (5)$$

$$W_N = \exp\left(\frac{-j2\pi}{N}\right),\ A_h = a_h \exp\left(-j\frac{4\pi}{\lambda}\right)R_h(t_0),$$

$$f_h = \left(\frac{2\omega r^T}{\lambda}\right)\left(\frac{N_f}{prf}\right)$$

where

$$\gamma_h = \left(\frac{\alpha r^T}{\lambda}\right)\left(\frac{N_f^2}{prf}\right), \beta_h = \left(\frac{\zeta r^T}{3\lambda}\right)\left(\frac{N_f^3}{prf^2}\right), \quad (6)$$

$$\phi_h = \left(\frac{\varsigma r^T}{\lambda}\right)\left(\frac{N_f^4}{prf^3}\right)$$

where A_h is the amplitude, f_h is frequency, γ_h is chirp rate, β_h and ϕ_h are derivates of the chirp rate.

4. MODELS FOR RIC

MDCFT and MFCFT algorithms are employed to process the incoming signal for third- and higher-order terms after migration through the resolution cell and create the final ISAR image.

A. MDCFT FOR CUBIC CHIRPS.

Given is the MDCFT for cubic chirp signals [7]

$$Z(m,l,k) = \frac{1}{\sqrt{N_f}} \sum_{n=0}^{N_f-1} z(n) W_{N_f}^{mn+(l/N_f)n^2+(k/N_f^2)n^3} \quad (7)$$

$$0 \le m,l,k \le N_f - 1$$

Here, z(n) -is chirp signal, k denote derivative of chirp rate, and m,l,k are approximated as

$$m \in (0,1...N_f - 1); l \in \left(0, \frac{1}{N_f} ... \frac{N_f - 1}{N_f}\right); \quad (8)$$

$$k \in \left(0, \frac{1}{N_f^2} ... \frac{N_f - 1}{N_f^2}\right)$$

Following are the procedures for using MDCFT-based ISAR imaging for cubic chirps:

Apply " (7)" to "(5)" to get

$$S(m,l,k) = \frac{1}{\sqrt{N_f}} \sum_{n=0}^{N_f-1} S(n) W_{N_f}^{mn+(l/N_f)n^2+(k/N_f^2)n^3} \quad (9)$$

S(m,l,k) is the MDCFT of S(n) and will produce a Doppler image in 3D. The accumulation of

energy along the axes of l and k will result in the formation of IDI(m), a 3D image as

$$I_{DI}(m) = \left| \sum_{l} \sum_{k} S(m,l,k) \right| \tag{10}$$

Image for the cubic chirp signal is created by combining the images from each range bin.

B. MFCFT FOR FOURTH-ORDER PHASE TERMS

The MFCFT expression for fourth-order phase terms is given by

$$Y(m,l,k,o) = \frac{1}{\sqrt{N_f}} \sum_{n=0}^{N_f-1} x(n) W_{N_f}^{mn+(l/N_f)n^2+(k/N_f)n^3+(o/N_f)n^4} \tag{11}$$

$$0 \le m,l,k,o \le N_f - 1$$

Here, m, l remains the same and $k \in \left(0, \frac{1}{N_f} \ldots \frac{N_f-1}{N_f}\right)$; $o \in \left(0, \frac{1}{N_f} \ldots \frac{N_f-1}{N_f}\right)$

The steps for ISAR imaging based on MFCFT are implemented by applying "(11)" to "(5)" to get

$$S(m,l,k,o) = \frac{1}{\sqrt{N_f}} \sum_{n=0}^{N_f-1} s(n) W_{N_f}^{mn+(l/N_f)n^2+(k/N_f)n^3+(o/N_f)n^4} \tag{12}$$

The other steps are the same as discussed in section IV-A. Due to the postponed treatment of the Nf exponent, the suggested method becomes increasingly more efficient as higher and higher-order terms are taken into account.

5. SIMULATION RESULTS

For simulation, a ship target with 32 scattering points is considered and is depicted in Figure 6a. Figures. 6.b to 6.f, shows the pictures produced by the RD, RID, and RIC approaches are displayed, respectively.

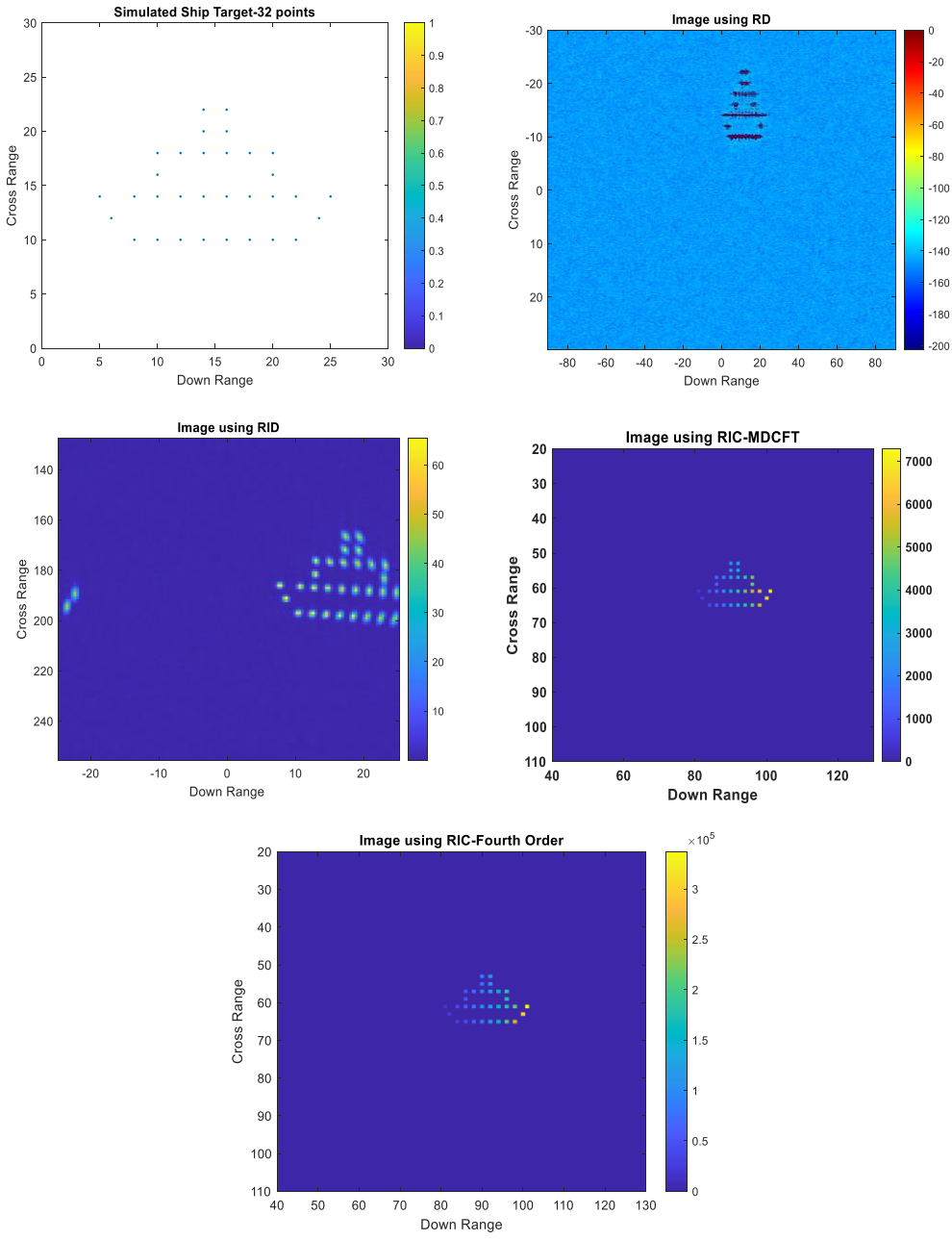

Fig.6.a. Simulated ship target b. Image using RD c. RID d. RIC-MDCFT e. RIC-MFCFT Fourth-order

The Figures make it obvious that the hot spots found using the suggested method outperform all the other algorithms.

Table.1: Comparison of CRR for different methods

Resolution	RD	RID	RIC-MDCFT	RIC-Fourth Order
DRR(m)	1	1	1	1
CRR(m)	1.84	1.21	1.05	1.05

Table 1 shows the DRR and CRR obtained for all the methods. From the Table, it is clear that the downrange resolution is 1meter, which is calculated using equation 1, and the cross-range resolution is calculated using equation 2 and is found to be better for the proposed method.

6. CONCLUSION

This work discusses ISAR imaging for higher-order phase signals utilizing MFCFT. When utilizing MFCFT for Fourth-order phase terms, the image quality is superior to that of more traditional approaches, and the calculation time is also considerably decreased. As higher and higher-order terms must be taken into account, this strategy will be shown to be more efficient.

References

[1] Mark.R, et.al., “Principles of Modern Radar”, Publishing.: Scitech Pub,Edison,NJ, 2010.

[2] Y. Wang and B. Zhao, "Inverse synthetic aperture radar imaging of nonuniformly rotating target based on the parameters estimation of multicomponent quadratic frequency-modulated signals", IEEE Sensors J, Vol. 15, No.7, pp. 4053-4061, 2015.

[3] Can Liu, et.al., “ISAR Imaging of Non-Stationary Moving Target Based on Parameter Estimation and Sparse Decomposition”, Remote Sensing, Vol-15, No-9, 2023.

[4] Y. Wang and Y. Jiang, "ISAR imaging of maneuvering target based on the L-class of fourth-order complex-lag PWVD", IEEE Trans. Geosci. Remote Sens., Vol. 48, No. 3, pp. 1518-1527, 2010.

[5] Z. Liu and Y. Jiang, "A novel Doppler frequency model and imaging procedure analysis for bistatic ISAR configuration with shore base transmitter and shipborne receiver", IEEE J Sel. Topics Appl. Earth Observ. Remote Sensing, Vol. 9, No. 7, pp. 2898-3000, 2016.

[6] Fengkai Liu, et.al., “Fast ISAR imaging method for complex manoeuvring target based on local polynomial transform-fast chirp Fourier transform”, IET Radar Sonar & Navigation, Vol. 15, Issue.6, pp.666-676, 2021.

[7] Xiang-Gen Xia,”Discrete Chirp Fourier Transform and its Application to Chirp Rate estimation”, IEEE Trans. Signal Processing, Vol.48, No.11, pp.3122-3133, 2000.

[8] Marco M, et.al., “Statistical CLEAN Technique for ISAR Imaging”, IEEE Trans on Geoscience and Remote Sensing”, Vol.45, No.11, pp.3552-3560, 2007.

[9] Y. Li, et.al., "Inverse synthetic aperture radar imaging of ship target with complex motion", IET Radar Sonar Navigation, Vol.2, No.6, pp. 395-403, 2008.

[10] Anitha.G,” Design of a new algorithm MFCFT using ISAR imaging to improve the Cross-Range Resolution and Computation Time”, YMER Journal, Vol.21, Issue-5,pp.854-862, 2022.